A STUDY OF LIGHTNING EFFECT ON A PV SYSTEM

MUHAMMAD AZIIM BIN BAHARAM

**BACHELOR OF ELECTRICAL ENGINEERING WITH HONOURS
UNIVERSITI TEKNIKAL MALAYSIA MELAKA**

2024

A STUDY OF LIGHTNING EFFECT ON A PV SYSTEM

MUHAMMAD AZIIM BIN BAHARAM

A report submitted
in partial fulfilment of the requirements for the degree of
Bachelor of Electrical Engineering with Honours

Faculty of Electrical Technology and Engineering
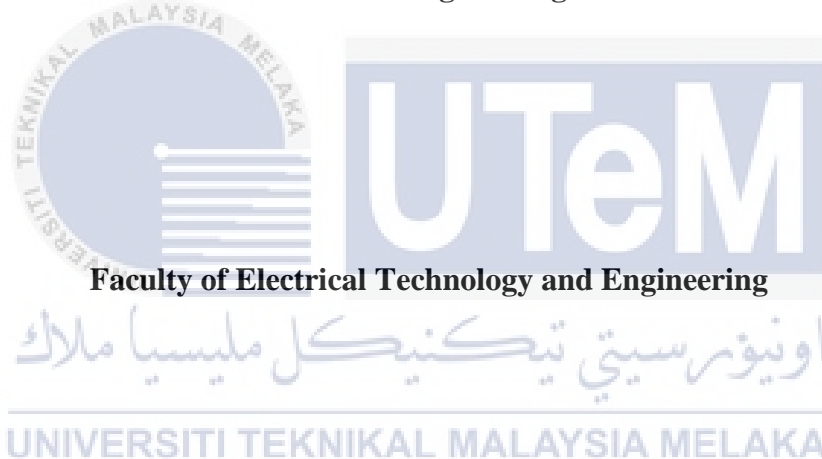
UNIVERSITI TEKNIKAL MALAYSIA MELAKA

2024

DECLARATION

I declare that this thesis entitled "A Study of Lightning Effect on a PV System is the result of my own research except as cited in the references. The thesis has not been accepted for any degree and is not concurrently submitted in the candidature of any other degree.

Signature   :

Name   :   Muhammad Aziim bin Baharam

Date   :   12 June 2024
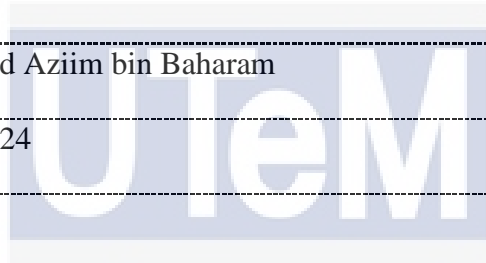
APPROVAL

I hereby declare that I have checked this report entitled " A Study of Lightning Effect on a PV System ", and in my opinion, this thesis fulfils the partial requirement to be awarded the degree of Bachelor of Electrical Engineering with Honours

Signature   :

Supervisor Name   :   Anis Niza binti Ramani

Date   :   12 June 2024
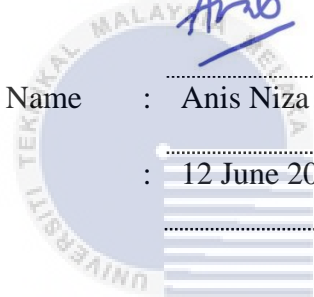
DEDICATIONS

This report is dedicated to my parents, who sacrificed everything to ensure that I would have

the opportunity of an education, for their unending love, support and encouragement. Thank

you for encouraging me to strive for the stars. I have a lot of faith that this achievement will

make the dream come true that you had for me many years ago when you resolved to give

me the very finest education that you could possibly provide.

ACKNOWLEDGEMENTS

ABSTRACT

It's widely known that Malaysia's solar photovoltaic systems are vulnerable to lightning strikes due to their installation in open areas with high radiation and lightning density. Lightning strikes can damage the electrical components of these systems, leading to electromagnetic interference and efficiency losses. To study this, a photovoltaic module was simulated and tested under normal and lightning conditions using COMSOL Multiphysics software. Two cases were examined: the effect of different current injection points and various solar cell materials on magnetic field and flux density. Results indicate that under lightning conditions, electromagnetic interference is notably higher compared to normal conditions. Moreover, the placement of current injection points significantly influences electromagnetic interference, impacting induced currents during lightning exposure. Additionally, there's a minor impact on electromagnetic interference from changes in solar cell materials, including Polycrystalline Silicon, Monocrystalline Silicon, and Thin-Film (Gallium Arsenide).

3

ABSTRAK

Umum mengetahui bahawa sistem fotovoltaik solar Malaysia terdedah kepada sambaran petir kerana pemasangannya di kawasan terbuka dengan sinaran tinggi dan kepadatan kilat. Sambaran petir boleh merosakkan komponen elektrik sistem ini, yang membawa kepada gangguan elektromagnet dan kehilangan kecekapan. Untuk mengkaji ini, model fotovoltaik telah disimulasikan dan diuji dalam keadaan normal dan kilat menggunakan perisian COMSOL Multiphysics. Dua kes telah diperiksa: kesan titik suntikan arus yang berbeza dan pelbagai bahan sel suria pada medan magnet dan ketumpatan fluks. Keputusan menunjukkan bahawa dalam keadaan kilat, gangguan elektromagnet adalah lebih tinggi berbanding keadaan biasa. Selain itu, penempatan titik suntikan semasa dengan ketara mempengaruhi gangguan elektromagnet, memberi kesan kepada arus teraruh semasa pendedahan kilat. Selain itu, terdapat kesan kecil pada gangguan elektromagnet daripada perubahan dalam bahan sel suria, termasuk Polihabluran Silikon, Monocrystalline Silicon dan Thin-Film (Gallium Arsenide).

TABLE OF CONTENTS

اونيۏرسيتي تيكنيكل مليسيا ملاك

UNIVERSITI TEKNIKAL MALAYSIA MELAKA

6

LIST OF TABLES

LIST OF FIGURES

LIST OF SYMBOLS AND ABBREVIATIONS

PV	-	Photovoltaic
LPS	-	Lightning Protection System
V	-	Voltage
A	-	Ampere
RE	-	Renewable Energy
NEM	-	Net Energy Metering
Mono-SI	-	Monocrystalline Solar Panel
Poly-SI	-	Polycrystalline Solar Panel
MPO	-	Maximum Power Output
DC	-	Direct Current
AC	-	Alternating Current
3D	-	3-dimension
W	-	Watt
LLS	-	Lightning Location System
EMTP-RV	-	ElectroMagnetic Transients Program
PCS	-	Power Conditioning System
m	-	Meter
k	-	Kilo
VSTL	-	Virtual Surge Test Lab
FDTD	-	Finite-Difference Time-Domain
PSCAD	-	Power Systems Computer Aided Design
EMTDC	-	Electromagnetic Transients including DC
EMC	-	Electromagnetic Compatibility
EMI	-	Electromagnetic Interference

CHAPTER 1

INTRODUCTION

1.1 Background

Solar photovoltaic (PV) systems have risen to prominence as a sustainable and efficient solution for harnessing renewable energy. However, the growing adoption of PV technology necessitates a nuanced understanding and proactive measures to address associated challenges, with the impact of lightning strikes being a significant concern. The discourse underscores the critical importance of implementing protective measures to effectively mitigate potential damage and ensure the robustness of solar energy infrastructure. In light of the increasing reliance on PV systems, a comprehensive comprehension of the dynamics surrounding lightning-induced effects is imperative for advancing the resilience and reliability of renewable energy technologies.

A pivotal facet in comprehending the repercussions of lightning on PV systems lies in the meticulous examination of transient currents and voltages elicited during a lightning strike. A study expressly dedicated to observing these transient phenomena within the context of a solar PV system [1]. The research endeavors to discern and analyze these transient dynamics, serving as a fundamental step toward identifying vulnerabilities and potential weak points inherent in the system. The insights garnered from such investigations prove instrumental in informing the development of strategic and efficacious protective measures. This deliberate approach to understanding the nuanced transient behavior induced by lightning strikes is paramount for fortifying the resilience and reliability of solar PV systems in the face of adverse environmental conditions.

The amalgamation of solar PV systems with energy storage solutions, notably batteries, introduces a layer of intricacy that warrants thorough examination. Delves into the investigation of lightning-induced voltage effects on a hybrid solar PV-battery energy storage system, considering the presence of surge protective devices [2]. This

scholarly inquiry highlights the necessity for a holistic and discerning approach to protection strategies, particularly in the realm of hybrid energy systems. The intricate interplay of components within such systems amplifies the importance of safeguarding measures against potential damage stemming from lightning strikes. The findings underscore the imperative for nuanced protective methodologies, acknowledging the complexities inherent in hybrid solar PV-battery energy storage configurations to ensure the resilience and integrity of these integrated energy solutions.

The optimal performance of PV modules stands as a pivotal determinant for the overall efficiency of solar PV systems. Systematically investigates the direct impact of lightning strikes on photovoltaic modules, elucidating the potential consequences such events bear on the system's power generation ratio [3]. This discerning exploration underscores the vulnerability of critical components within PV installations to damage induced by lightning strikes. The study accentuates the imperative need for proactive and robust protective measures, emphasizing their role in preserving the long-term performance and sustainability of photovoltaic installations. Acknowledging the intricate relationship between lightning-induced effects and PV module functionality becomes paramount for the continued advancement of resilient and high-performing solar energy systems.

A comprehensive viewpoint is afforded through an in-depth study concentrated on lightning protection systems, delineating the intricacies of lightning damage mechanisms and fundamental principles of protection [4]. A nuanced comprehension of the underlying physics and principles governing lightning strikes proves indispensable in the formulation of efficacious protection systems. This study, by delving into the intricacies of lightning-induced damage and elucidating foundational protective principles, contributes substantive insights. The knowledge derived from this investigation is instrumental in devising proactive measures aimed at safeguarding PV systems against the potential adversities posed by lightning strikes. The study underscores the significance of an informed and strategic approach to lightning protection, accentuating its role in fortifying the resilience and longevity of PV installations.

12

Addressing and mitigating the adverse impacts of lightning strikes on PV systems necessitates the formulation and adherence to stringent design guidelines. Advocates for an initial phase of comprehensive background research into the nature of lightning, accentuating the pivotal importance of understanding its inherent characteristics and mechanisms [5]. This underscores the necessity for a proactive approach during the design phase, where the implementation of protective measures is tailored to align with the specific risks posed by lightning in a given geographical location. By advocating for a foundational understanding of lightning's intricacies, this reference underscores the significance of informed decision-making in the design process, reinforcing the resilience and longevity of PV systems against the potential disruptions induced by lightning events.

In conclusion, the amalgamated findings from these studies unequivocally indicate that lightning strikes can exert a deleterious influence on solar PV systems. Whether discerned through the observation of transient currents and voltages, the scrutiny of hybrid systems, or an in-depth understanding of the direct impact on photovoltaic modules, a consistent thread emerges: the imperative role of protective measures. The deliberations on lightning protection systems and design guidelines underscore the necessity for a comprehensive and proactive approach to mitigate potential damage. As the global trajectory pivots towards increased reliance on renewable energy, these collective studies underscore the critical significance of continual research endeavors and the implementation of robust protective measures. This strategic approach is indispensable to ensure the resilience and enduring viability of solar photovoltaic systems in confronting challenges induced by lightning events.

1.2 Motivation

The global energy landscape faces a critical challenge marked by a widening gap between escalating electricity demand and depleting fossil fuel reserves. To address this, a crucial shift towards alternative and sustainable energy sources is imperative. Renewable technologies such as solar, wind, hydropower, geothermal, and biomass offer environmentally friendly solutions, harnessing energy from naturally replenished

sources. This transition not only mitigates the environmental impact of traditional energy sources but also promotes energy security and resilience. Investments in research, development, and infrastructure are essential to make these technologies more efficient and widely accessible, enabling a sustainable and balanced global energy future.

In November 2016, the Malaysian government took a significant step towards promoting the adoption of Renewable Energy (RE) by introducing the Net Energy Metering (NEM) Scheme. This initiative, with a quota allocation of 500 megawatts (MW) until the year 2020, aims to incentivize and facilitate the integration of renewable energy sources into the country's energy mix. Under the NEM Scheme, individuals and businesses are encouraged to install renewable energy systems, such as solar panels, on their premises. The surplus energy generated by these systems can be fed back into the grid, allowing consumers to receive credits for the excess electricity produced. This not only promotes the use of clean and sustainable energy but also empowers citizens to actively participate in the nation's transition towards a more environmentally friendly and energy-efficient future.

The proposed project seeks to fill a crucial knowledge gap by conducting simulations to analyze the impact of lightning on PV panels. By simulating the lightning effect, the project aims to provide valuable insights into induced overvoltage and current, which are essential factors for optimizing the design of PV panels and ensuring their reliability. Understanding how lightning affects PV systems is critical for developing robust and resilient solar energy infrastructure. The simulation results will contribute to improved design strategies, helping to enhance the overall performance and durability of PV panels, thereby advancing the efficiency and reliability of solar energy generation technologies.

1.3 Problem Statement

Solar energy in Malaysia has substantial potential for growth in increasing its share of renewable energy in the country's power generation mix. However, it also faces significant risks. Due to installations in wide-open areas with high radiation and frequent lightning, photovoltaic (PV) modules in Malaysia are prone to lightning strikes. These strikes inject large transient currents into PV modules, exceeding safe limits and causing transient overvoltages that degrade electrical insulation within the equipment. This can lead to electromagnetic interference (EMI), potentially damaging the PV modules and other electrical components. Such interference can also impair the performance of the PV system, reducing electricity production. Since there is currently no specific standard for lightning protection systems (LPS) against EMI for PV modules during lightning events, it is crucial to conduct research and simulations on EMI under both normal and lightning conditions. This effort aims to ensure that simulated results adhere to standard limits, thereby maintaining EMI within safe ranges.

1.4 Objective

1. To develope a 3D solar PV module using Comsol Multiphysics.

2. To simulate the interference of magnetic field and magnetic flux density under normal and lightning condition using Comsol Multiphysics.

3. To analyze the effect of different electric current injection points and solar cell material toward magnetic field and magnetic flux density using Comsol Multiphysics.

15

1.5 Scope

The objective of this study is to enhance the understanding of material properties and lightning behavior concerning PV modules. This is accomplished by developing a model of a PV module in COMSOL Multiphysics software, adhering to proposed dimensions. Electric current is injected into these models at two positions: the middle and corner of the PV module. Models are then subjected to two conditions: normal and lightning. Additionally, three types of solar cell materials—Polycrystalline Silicon, Monocrystalline Silicon, and Thin-Film (Gallium Arsenide)—are analyzed. The simulation takes place within a sphere of air domain with a suggested radius. The focus of the results lies in comparing the effects of different injection points of electric current and various solar cell materials on electromagnetic interference (EMI), encompassing magnetic field and magnetic flux density. These simulated results are compared against the BSI Standard of Electromagnetic Compatibility (EMC), specifically BS EN 61000-4-9, to ascertain compliance with allowable limits.

16
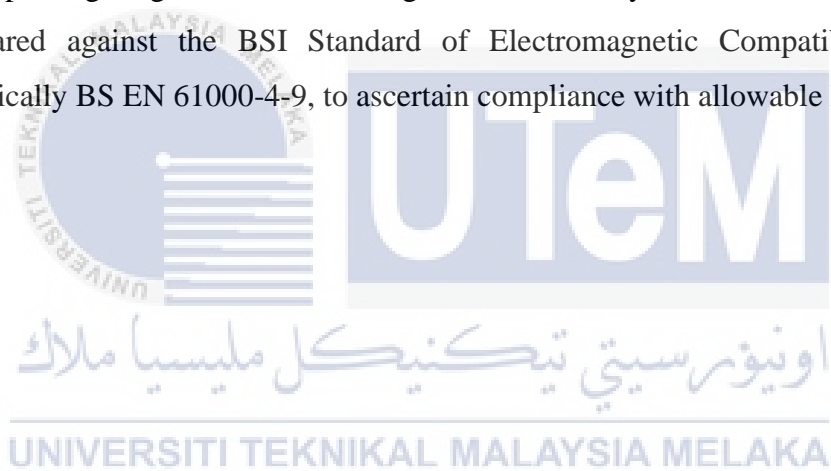
CHAPTER 2

LITERATURE REVIEW

2.1 Overview of Solar PV Panel in Malaysia

Malaysia, endowed with consistent and plentiful sunlight throughout the year, is presently witnessing a substantial increase in the integration of solar PV panels. Constructed with semiconductor materials such as silicon, these panels efficiently convert sunlight into electrical energy, presenting a clean and sustainable alternative to conventional fossil fuels. There are three varieties of solar panels accessible in Malaysia, each with its own set of advantages to cater to your individual needs. The following enumerates the diverse types of solar panels.

Monocrystalline Solar Panels, also known as Mono-SI, distinguish themselves in the realm of solar energy generation through a combination of high-power output, space efficiency, and extended lifespan. These panels offer an optimal solution for those seeking maximum energy production within limited space, as their compact design allows for effective utilization of available surface areas. One notable advantage of monocrystalline panels lies in their exceptional durability, surpassing other types of solar panels. These panels demonstrate robust construction, making them less susceptible to environmental factors and ensuring a prolonged lifespan for solar installations. Moreover, monocrystalline panels exhibit a remarkable resistance to high temperatures. This characteristic enhances their reliability and performance, particularly in regions with elevated ambient temperatures or during peak sunlight exposure. While the benefits of monocrystalline solar panels are evident, it's essential to acknowledge that they are often associated with a higher upfront cost compared to alternative panel types. However, the superior efficiency, longevity, and resilience of monocrystalline panels justify this initial investment, making them a prudent choice for those prioritizing reliability and long-term performance in their solar energy systems.

17

The second type of solar panel available in Malaysia is the Polycrystalline Solar Panel, denoted as Poly-SI. Distinct from its monocrystalline counterpart, the polycrystalline variant operates with a lower level of efficiency, occupies a larger footprint, and generally has a shorter lifespan. While these characteristics may be perceived as trade-offs, polycrystalline solar panels come with a significant advantage — their cost-effectiveness. This makes them an appealing choice for individuals or businesses in Malaysia looking to optimize their investment in solar energy. The affordability of polycrystalline panels positions them as a viable option for those who prioritize upfront cost savings without compromising on the essential benefits of solar energy. Therefore, if your objective is to strike a balance between cost and solar energy adoption, polycrystalline solar panels offer a compelling solution in the Malaysian context.

The third variant in the realm of solar panels is represented by Thin-Film Solar Panels, showcasing distinctive features that set them apart from the aforementioned types. A fundamental contrast emerges in the composition of thin-film solar panels, which diverge from a single material source to incorporate a diverse array of materials. This unique characteristic contributes to the flexibility, lightweight nature, and portability that define thin-film panels. While these attributes make thin-film solar panels an intriguing option, a notable drawback must be considered—namely, their spatial requirements. Due to the design and construction, thin-film panels demand a significant amount of space, rendering them less practical for certain locations or applications where space is limited. Therefore, when contemplating the incorporation of thin-film solar panels, a meticulous evaluation of available space becomes imperative, ensuring alignment with the specific spatial considerations of the intended installation site.

2.2 Solar cells

A solar cell, commonly referred to as a photovoltaic cell, functions to convert sunlight into electricity by harnessing the photovoltaic effect. Primarily composed of semiconductor materials, notably silicon, these cells initiate the generation of an electric current upon exposure to sunlight. This process unfolds as photons in sunlight

energize electrons within the semiconductor material, leading to the production of electricity. The ensuing electric current is captured by metal contacts, establishing a functional electric circuit. Methodically integrated into solar panels, these cells play a pivotal role in sustainable energy generation across various applications, spanning from residential installations to expansive solar farms. This technological advancement significantly contributes to the fostering of an environmentally conscientious and sustainable energy landscape.

2.2.1 The Operational Mechanism of Photovoltaic Cells.

The fundamental component of a solar energy generation system is the PV cell, meticulously crafted to efficiently convert sunlight into electrical energy. Functioning as a p-n junction device, the designation "n-type" signifies electrons introduced by donor impurity atoms, resulting in a negative charge, while "p-type" denotes positively charged holes generated by acceptor impurity atoms. This classification corresponds with the illustration in Figure 2.1 of a PV structure [6,7,8].
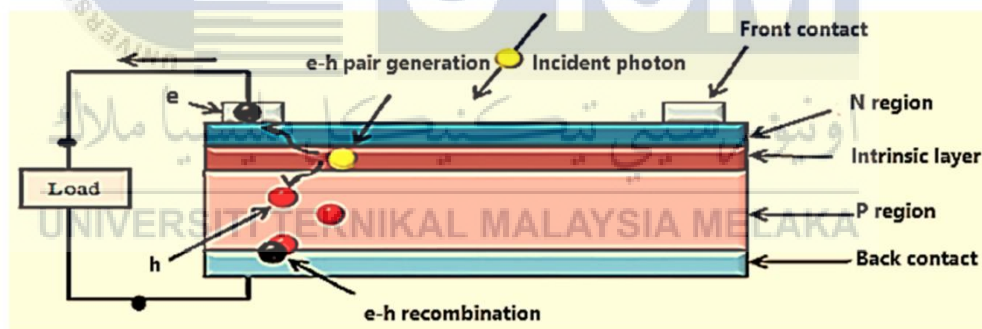
Figure 2.1 A PV cell with a p-n junction [6,7,8]

The operation of solar cells hinges on the photovoltaic effect, an occurrence that can be classified into three fundamental processes [9,10,11]. The generation of charge carriers, in the form of electron-hole pairs, occurs through the absorption of photons in a p-n junction electronic semiconductor. When a photon possesses energy ($E = h\nu$) greater than the gap energy 'Eg' of the doped semiconductor material, it raises an electron from the valence band '$E\nu$' to the conduction band 'Ec,' creating a hole in the valence level. The excess photon energy ($h\nu-h\nu0$) imparts additional kinetic energy to the electron or hole, where '$h\nu0$' denotes the minimum energy or work function of the

19

semiconductor necessary to generate an electron-hole pair. This work function corresponds to the energy gap, and any surplus energy dissipates as heat within the semiconductor [12,13].

1. Subsequent to this step, the charge carriers generated by light undergo separation. Within an external solar circuit, holes have the capability to migrate away from the junction through the p-region, while electrons exit through the n-region, traversing the circuit before recombining with the holes.

2. Eventually, the isolated electrons can be employed to energize an electric circuit. Upon concluding their trajectory through the circuit, the electrons reunite with the holes.

The n-type layer must be configured to be thinner than the p-type layer. This design ensures that electrons can efficiently traverse the circuit, generating current swiftly before recombining with the holes. Additionally, an anti-reflective coating is applied over the n-layer to mitigate surface reflection and augment the transmission of light to the semiconductor material.

All the aspects outlined in this section will be expounded upon in greater detail in the subsequent sections.

2.2.2 Solar Cell Panels

Solar panels consist of multiple solar cells interconnected in both series and parallel configurations to achieve a specific power output. Utilizing a single PV cell is often impractical for most applications due to its limited voltage production, typically around 0.5 V. To overcome this limitation, multiple cells, such as six cells, can be connected in series, where the total voltage is assumed to be the sum of individual cell voltages, resulting in an ideal 3 V (6×0.5 V). Moreover, cells connected in series can be arranged in parallel to enhance current capacity. For instance, if the six cells collectively generate 2 A, a series-parallel configuration with twelve cells is anticipated to produce 4 A at 3 V [14].

2.2.3 Elements of Solar Power System

A PV system comprises a solar panel, supercapacitor, and inverter. The solar panel captures photon energy and converts it into electricity through the PV mechanism. The supercapacitor backup is employed to provide additional energy, particularly during sunny days. The generated DC power is then transformed into AC loads to render it suitable for household usage [15,16], as depicted in Figure 2.2.
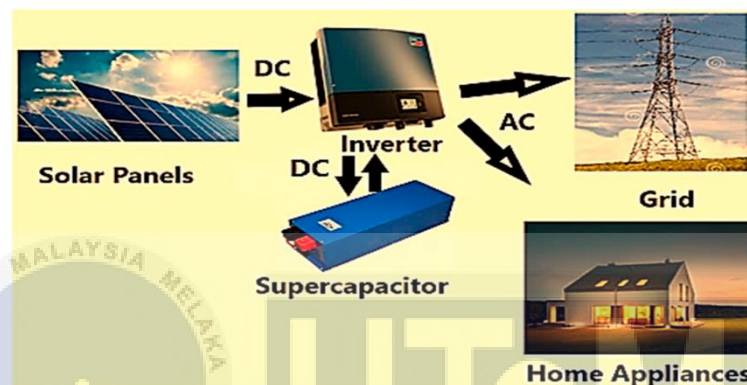
Figure 2.2 The fundamental elements of a PV system [15,16]

2.4 Categorization of Solar Photovoltaic Panels.

A PV device is a technology engineered to convert sunlight into electricity utilizing semiconductor cells [17,18]. These cells generate a current at a consistent voltage of 0.6 V per cell [19]. Typically, a solar panel comprises an array of these cells. Figure 2.3 illustrates the two primary types of panels: crystalline and thin-film. Crystalline panels encompass monocrystalline and polycrystalline varieties, while thin-film panels are further categorized into amorphous, cadmium telluride, copper indium diselenide, and copper indium gallium diselenide types.

PV panels are classified according to their core materials, output efficiency, resistance, and other factors. Figure 2.4 presents a condensed comparison of PV solar panels, drawing information from various articles or references.

21
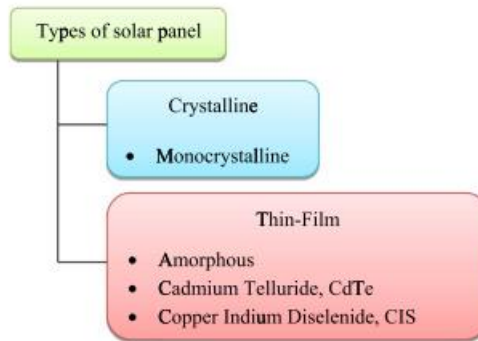
Figure 2.3 Classifications of PV Panels [20-22]

	Monocrystalline	Polycrystalline	Thin Film Amorphous	CdTe	CIS/CIGS
Material	Silicon	Silicon	Silicon	Cadmium and Telluride	Copper, Indium, Gallium/Selenium
Cell efficiency	25.00%	20.40%	13.40%	18.70%	20.40%
Module efficiency	15–20%	13–16%	6–8%	9–11%	10–12%
Area required for 1 kWp	6–9 m^2	8–9 m^2	13–20 m^2	11–13 m^2	9–11 m^2
Temperature resistance	Performance degrade at high temperatures	Less temperature resistant than monocrystalline	Tolerates extreme heat	Low impact on performance	
Warranty	25 years	25 years	10–25 years	-	
Widely used	Grid-connected PV systems	Off-grid connected PV systems (Stand-alone)	More in off-grid connected PV systems (Eg: Portable solar chargers)		

Figure 2.4 Classifications of PV Panels [23-28]

2.5 Lightning Occurence

Lightning, a prevalent natural phenomenon observable from outer space, is also recognized as one of the most perilous occurrences for humanity due to its potential catastrophic effects [29]. Typically, lightning manifests as a transient, high-current electric discharge with a path length measured in kilometers. The air, serving as an insulator between positive and negative charges in the cloud and between the cloud and the ground, loses its insulating capacity when opposing charges accumulate sufficiently. This breakdown leads to the rapid discharge of electricity known as lightning [30,31]. Figure 2.5 provides an overview of the primary types of lightning within the context of lightning occurrences.

22

The density of lightning occurrences is characterized by two parameters [32]:

1. Isokeraunic level:
   o It denotes the average annual incidence of thunderstorm days or hours in a particular location and is commonly the principal source of information regarding lightning density in numerous countries.
   o However, its precision is not very high, and at times, it may give a misleading impression of the lightning density in a particular region.
   o In contrast, satellite data offers the total flash density for a specific area.

2. Ground Flash Density:

Ground flash density is defined as the annual number of lightning flashes per square kilometer ($km^2 \ yr^{-1}$) [33]. Key characteristics of ground flash density [34,36] encompass:
   • Variation observed across geographical regions and within the same region, with the potential for multiple ground terminations.
   • Values that might exceed the predicted data obtained from the Lightning Location System (LLS).

Recording ground flash density can be accomplished through diverse means, including lightning flash counters, LLS, and satellite-based optical or radio-frequency radiation detectors [34,36,37].

Types	Description
Intra to cloud	Occurs between opposite charges within the thunderstorm cloud.
Cloud to cloud	Occurs between opposite charges in the cloud and another cloud.
Cloud to ground	Occurs between opposite charges in the cloud and on the ground.
Ground to cloud	Occurs in the reverse direction

Figure 2.5 Types of Lightning [33,34]

In Germany, depicted in the statistical data presented in Figure 2.7, it is indicated that 26% of damage to PV systems results from lightning strikes and surges. This percentage might be even more prominent in countries situated near the equatorial regions. Figure 2.8 delineates the typical damage arising from a lightning strike, providing details on the affected components of PV systems. Lightning strikes and surges emerge as significant contributors to the decline in the efficiency of a PV system.
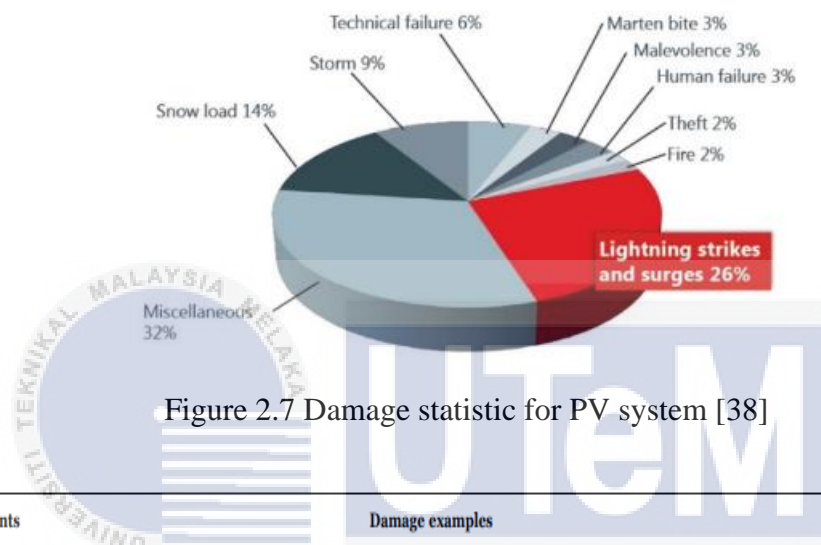
Figure 2.7 Damage statistic for PV system [38]

Components	Damage examples
PV modules	Defects on bypass diodes, broken glasses, and arcing at string ribbon.
Inverter and monitoring combiner boxes (Weather sensors)	All inputs and outputs include data communication/displays.
Cables	Holes in the insulation whereby the spark over from the mounting system and spark over into the soil.
Solar tracker	Communication, sensors, power supply, and drive train.
Security systems	Cameras, sensors, data communication, and theft protection.

Figure 2.6 Damage examples for PV system [39]

2.6 Lightning Protection System (LPS) Scheme

The Lightning Protection System (LPS) of a photovoltaic (PV) system is designed to protect PV panels, inverters, and related equipment from lightning damage. These systems usually incorporate ground electrodes, bonding conductors, and lightning rods [40].

The lightning rods, also known as air terminals, are installed on the roofs or elevated locations of PV systems. Bonding conductors within these terminals are tasked with conducting electrical energy from lightning strikes to the ground. Typically made of

24

copper or aluminum, these bonding conductors connect the lightning rods to ground terminals, which are positioned in the ground or suitable locations. This setup effectively channels the electrical energy from lightning strikes into the earth, ensuring the safety of the PV system and the structure it serves.

Developers primarily prioritize internal Lightning Protection Systems (LPS) due to their higher efficiency and cost-effectiveness compared to external LPS [41]. Internal LPS involves installing Franklin Rods, commonly known as lightning rods, either connected (non-isolated system) or not (isolated system) to the PV module. Selecting the optimal LPS approach entails comprehensive studies on PV system characteristics, lightning behavior, and electromagnetic compatibility (EMC), all while adhering to the BSI Standard of Electromagnetic Compatibility (EMC).

2.7 Electromagnetic Compatibility (EMC) Analysis

Electromagnetic Compatibility (EMC) analysis is a structured evaluation method employed to assess and guarantee that electronic and electrical devices, systems, and equipment can function together without disrupting each other's operations in the presence of electromagnetic fields.

EMC analysis aims to pinpoint potential electromagnetic interference (EMI) concerns that might emerge when multiple devices or systems are close or interconnected. Through comprehensive EMC analysis, engineers can devise and create products that meet the necessary electromagnetic compatibility standards, guaranteeing their dependable performance and adherence to regulatory mandates [42].

2.7.1 Electromagnetic Interference (EMI)

When lightning strikes a PV system, it may trigger a phenomenon referred to as EMI. This occurs due to the high-frequency electrical energy generated by lightning strikes, disrupting the normal functioning of electronic equipment. EMI can result in various

25

problems within a PV system, such as power outages, harm to PV panels, and damage to inverters. Additionally, false alarms and malfunctions in other connected electronic devices may occur.

The impact of EMI on PV systems during lightning strikes has been extensively studied. As per one research finding, EMI can cause temporary power interruptions in PV systems when lightning strikes, as the high-frequency electrical energy from the lightning can disrupt the normal functioning of PV panels and inverters [43]. Furthermore, it was noted that EMI has the potential to harm PV panels and inverters, thereby reducing the overall efficiency of the PV system.

An additional study found that EMI could lead to false alarms and operational malfunctions in other electrical devices linked to the PV system. The research indicated that lightning strikes may generate significant induced currents that propagate through power lines, inducing electromagnetic interference capable of impacting electronic equipment connected to a photovoltaic system [44].

2.7.2 Induced Current

An induced current arises in a conductor due to a changing electromagnetic field. External influences such as power lines or lightning strikes can give rise to induced currents. In photovoltaic systems, induced currents can occur during lightning strikes, as the high voltage and current induced by lightning can generate intense electromagnetic fields capable of initiating currents in the conductors of the PV system [45]. These induced currents pose a risk of damaging the system components or even causing a fire.

Induced currents stemming from nearby lightning strikes can exert influence on a photovoltaic system. These currents might traverse through the wiring of the PV system, potentially causing damage to inverters and other electronic components. Additionally, they can lead to fluctuations in power, disrupting the system's normal operation or causing it to cease functioning altogether.

2.8 BSI Standard of Electromagnetic Compatibility (EMC)

This specific standard pertains to testing and measurement methods for assessing immunity to conducted, common-mode disturbances within the frequency range of 0 Hz to 150 kHz. BS EN 61000-4-9 deals with evaluating and gauging equipment's resilience against disturbances induced by power-frequency magnetic fields [46]. It delineates precise test protocols and benchmarks to ascertain the performance and adherence of electronic and electrical equipment under such circumstances.

Following BS EN 61000-4-9 enables manufacturers and developers to verify that their products align with the necessary electromagnetic compatibility standards, thereby ensuring their dependability and effectiveness when exposed to power-frequency magnetic fields. Adherence to this standard reduces the likelihood of malfunctions, interference, or harm arising from electromagnetic disturbances.

This standard will be applied to the simulation results regarding magnetic field and magnetic flux density to verify whether they comply with the established limits.

2.9 Analysis Method

2.9.1 Effect of Lightning Strike on Different Part of Solar PV System

The aim of this research journal is to examine the transient current and voltage occurrences in a solar PV system upon lightning strike [47]. A model of the PV system was developed and simulated under two distinct striking locations: the DC side and the AC side, as depicted in Figure 2.8.
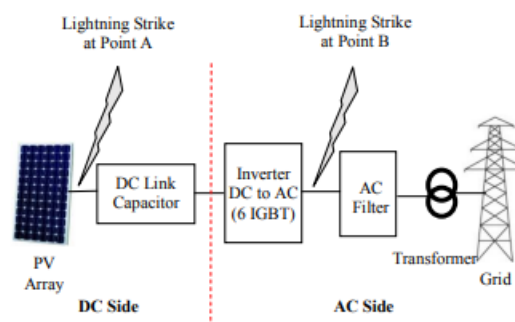
Figure 2.8 Lightning Strikes of DC and AC Side

27

The findings indicate that a transient current emerges at the nearest point to the lightning strike, carrying the same value as the injected lightning strike current [48]. Additionally, transient voltage manifests at the AC side regardless of the lightning strike point. Sample comparative values are illustrated in the figure below.

Lightning Impulse Current 0.25/100 μs							
I_{inject} (kA)	Strike at Point A				Strike at Point B			
	DC		AC		DC		AC	
	V_{max} (V)	I_{max} (kA)	V_{max} (MV)	I_{max} (kA)	V_{max} (V)	I_{max} (A)	V_{max} (MV)	I_{max} (kA)
20	704.26	20.00	1.33	6.66	704.54	43.00	1.33	6.66
40	704.17	40.00	2.66	13.31	94.36	35.97	2.66	13.31
60	704.15	59.95	4.00	19.99	704.6	71.52	4.00	19.97
80	704.15	79.92	5.33	26.63	188.59	47.02	5.33	26.63
100	733.10	99.89	6.66	33.28	235.69	48.26	6.66	33.28

Table 2.1 Sample Data of Transient Current and Transient Voltage during Lightning

According to this journal, the methodology can be adapted to develop a model and conduct analysis on the impact of different injection points of electric current on EMI using COMSOL Multiphysics software. However, there is a need to refine the model to concentrate solely on the PV module while injecting two types of electric current based on the proposed conditions. Subsequently, the simulation results will focus on magnetic field and magnetic flux density instead of transient current and voltage. These results will then be compared against the BSI Standard of Electromagnetic Compatibility (EMC) to determine which injection point yields outputs within the permissible range.

2.9.2 Comparative Analysis of Solar Cell Efficiency between Monocrystalline and Polycrystalline

The objective of this research journal is to investigate the influence of light intensity on the output power and efficiency of solar panels [49]. Employing a direct measurement approach, the study utilizes both a monocrystalline and a polycrystalline solar panel, each with an identical power capacity and a peak capacity of 50 Wp. Both panels are exposed to sunlight, and the solar energy produced is recorded hourly starting from 8:00 a.m., as outlined in Table 2.2. A comparison between the two materials is conducted in terms of efficiency. The findings indicate that monocrystalline solar panels exhibit higher efficiency, attributed to their greater solar energy production during peak sun hours.

No	Waktu	Monokristalin		Polykristallin		Temperatur (C^O)		It (Watt /m2)	Pin= I*Apa nel (watt)	Pout=V*I (Watt)		Efisiensi (η)=Pout/Pin(%)	
		V (Volt)	I (Ampere)	V (Volt)	I (Ampere)	T	Ta			Monokr istallin	Polykris tallin	Monok ristalin	Polykr istallin
1	08:00	18.58	0.72	18.5	0.84	28	28	313	112.99	13.37	15.54	11.83	13.75
2	09:00	18.35	0.84	18.4	0.75	34	32	384	139	15.41	13.8	11.08	9.92
3	10:00	19.69	1.01	19.83	0.97	36	35	425	153	19.88	19.23	12.99	12.56
4	11:00	19.4	1.01	19.37	0.97	38	34	373	135	19.59	18.78	14.51	13.91
5	12:00	18.25	0.81	18.34	0.72	38	36	288	104	14.78	13.2	14.21	12.69
6	13:00	19.53	1	19.56	0.94	38	36	445	161	19.53	18.38	12.13	11.41
7	14:00	19.82	0.98	19.99	0.9	37	35	415	150	19.42	17.99	12.94	11.99
8	15:00	19.58	0.63	19.88	0.62	36	32	284	103	12.33	12.32	11.97	11.9
9	16:00	19.4	0.76	19.8	0.76	34	34	329	119	14.74	15.04	12.38	12.63
10	17:00	19.28	0.82	19.46	0.86	32	31	384	139	15.8	16.73	11.36	12.03

Table 2.2 Output for Monocrystalline and Polycrystalline Solar Panel

The principles outlined in the journal can be employed to conduct analysis on various solar cell materials proposed in this project. However, there will be distinctions involving the manipulation of input values for electrical properties such as electrical conductivity, relative permittivity, and relative permeability for each material during simulation. This is necessary as the focus of the simulation results will be on magnetic field and magnetic flux density. Utilizing these EMI outcomes aids in evaluating which material is superior in terms of solar production efficiency.

2.10 Summary

Table 2.3 Summary of Literature Review

No	Year	Title	Sub-Topic	Content	Implementation
1	2022	PV System	Working Principles and Types of PV Cell	The operational principle of a photovoltaic (PV) cell involves converting sunlight into electrical energy. An overview of fundamental types of materials used in solar cells.	Choosing polysilicon, monocrystalline silicon, and thin-film for simulation and analysis purposes.
2	2010	Lightning	Type of lightning strike	Cloud to ground Ground to cloud Cloud to cloud Intra cloud	Selected cloud to ground to replicate as lightning strike during simulation.
3	2016	BSI Standard of Electromagnetic Compatibility	BS EN 61000-4-9	Standard values for magnetic field and magnetic flux density.	Compared with simulation output to verify the data is within allowable range.
4	2016	Analysis Method	Lightning strike on different part of PV system	To observe the transient current and voltage occurring in a solar PV system during a lightning strike.	Simulation concept
5	2019	Electromagnetic Compatibility (EMC)	Electromagnetic Interference (EMI)	Introduction on how external current of lightning affect the: 1) Magnetic Field 2) Magnetic Flux Density	Output of simulation
6	2012	Lightning Protection System (LPS)	LPS Scheme	A system engineered to protect PV installations from	Analysis

30

				the destructive impacts of lightning strikes.	

CHAPTER 3

METHODOLOGY

3.1 Introduction

This chapter outlines the experimental and descriptive methodologies utilized in this research. The methodology encompasses a general overview of the methods employed, data collection regarding standard limits and PV dimensions. It also entails the design of PV modules, parameter setup for magnetic field physics, simulation testing, outcome analysis, and the creation of a Gantt Chart.

3.2 Overview of Method
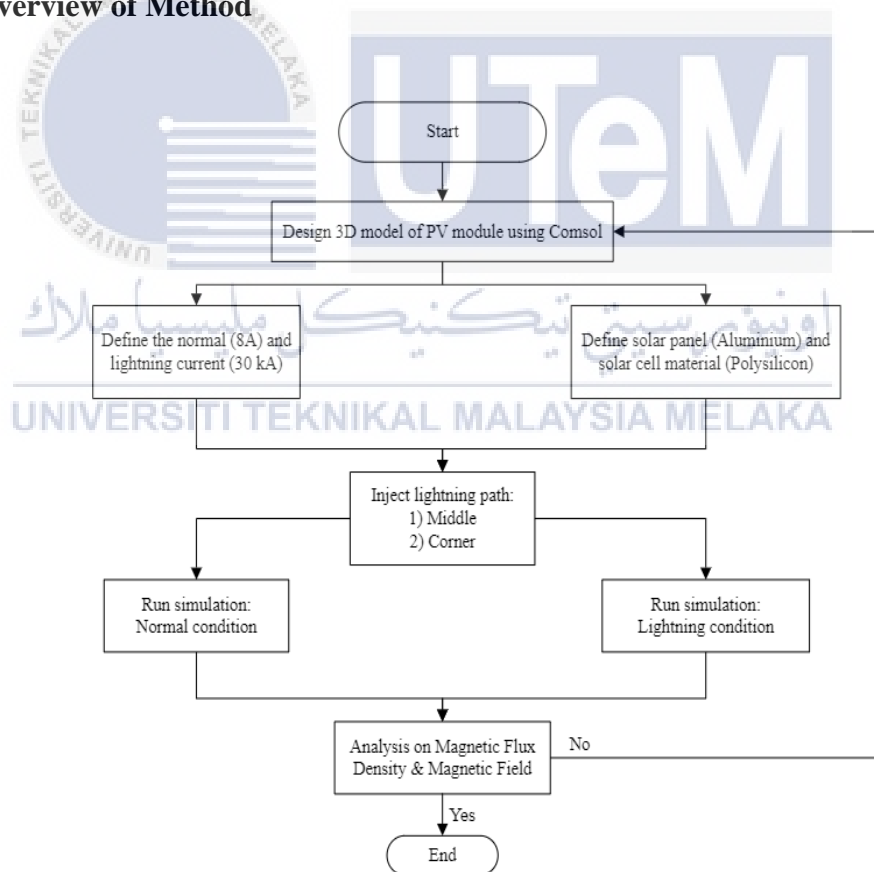
Figure 3.1 Flowchart of Methodology for Case 1
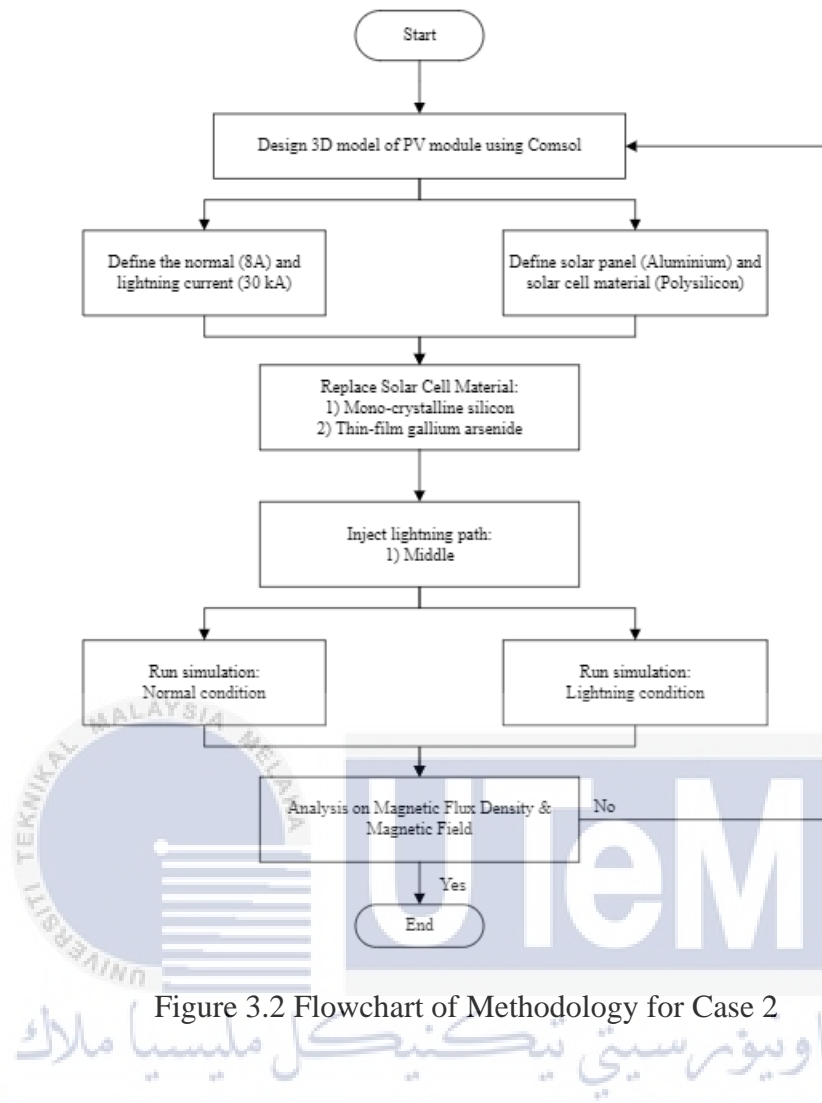
Figure 3.2 Flowchart of Methodology for Case 2

3.3 Defining the Standard Value of Magnetic Field and Magnetic Flux Density

This stage entails setting a standard point or initial measurement for these physical attributes. This standard value acts as a point of reference against which other measurements or computations can be evaluated, ensuring uniformity and precision within the realm of magnetism. According to the BSI Standard for Electromagnetic Compatibility (EMC), outlined in BS EN 61000-4-9, the established limits for magnetic field and magnetic flux density are delineated in the following table [46].

Electromagnetic Interference	Standard Limit
Magnetic Field	1000 A/m
Magnetic Flux Density	1260μT

Table 3.1 Standard Limit of BS EN 61000-4-9 [46]

The table presents standard limit values, which will serve as benchmarks for comparison with the simulation results. This comparison will ascertain whether the simulated outcomes fall within the acceptable range of safety.

3.4 Designing PV Module in Comsol Multiphysics Software

In this section, it's essential to initially pinpoint the specific requirements, including the types of components involved and the desired physical dimensions of the PV module [50]. Through research, it has been established that a PV module typically comprises a frame, solar cells, and a lightning rod. However, for the model, the lightning rod will be incorporated as it doesn't notably impact the objectives. Conversely, it has been determined that a residential panel includes a total of 60 solar cells [50]. The dimensions for the PV module are detailed in the table below.

Components	Design Specification (m)			
	Depth,ℓ	Width,w	Height,h	Quantity
Frame/ Panel	1	1.65	0.05	1
Solar Cell	0.15	0.15	0.02	60

Table 3.2 Physical Dimension of PV Module
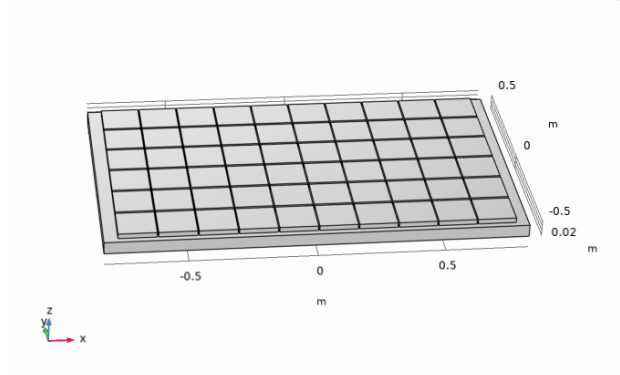
Figure 3.3 Aluminium Panel and 60 Solar Cells

3.5 Parameter Setup for Magnetic Field Physics

This section emphasizes three primary components to focus on: the frame, solar cell, and air domain sphere. Furthermore, the materials for these components have been proposed, and their respective electrical property values have been documented in the table below for simulation setup [51], [52].

Components	Materials	Electrical Properties		
		Electrical conductivity, σ (S/m)	Relative permeability, μ_r	Relative permittivity, ε_r
Frame/Panel	Aluminum	33.3e5	1.00000065	1
Solar Cell	Polycrystalline Silicon/Polysilicon	5e10	0.999837	4.5
	Monocrystalline Silicon/Monosilicon	3.14e-6	0.99837	11.7
	Thin-Film Silicon (Gallium Arsenide)	10e-6	0.999983	12.6
Sphere of Air Domain	Air	0	1	1

Table 3.3 Materials and Electrical Properties
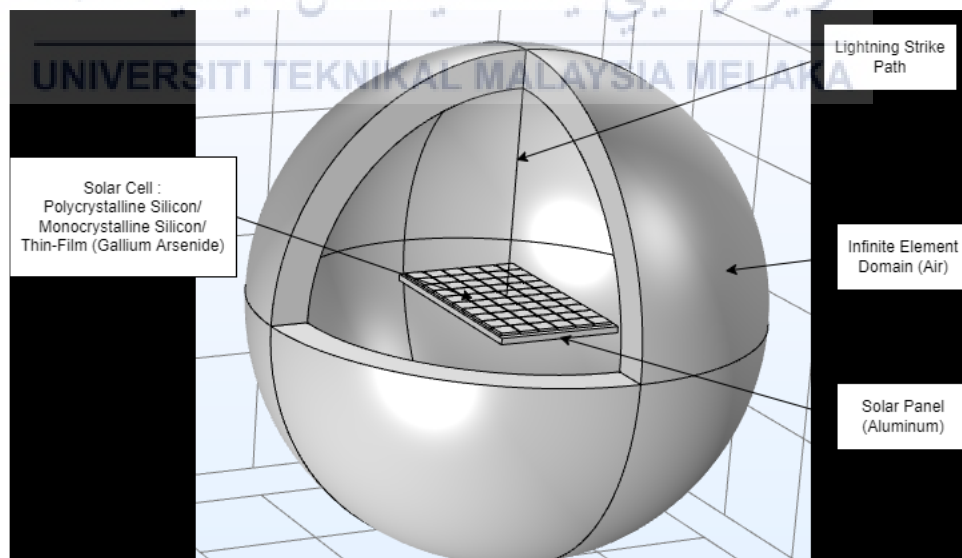
Figure 3.4 Material Section of 3D PV Module

Each component will have its electrical properties values assigned as inputs in the material section of the Comsol Multiphysics software. It's important to note that the proposed materials will be positioned according to their respective domains, as illustrated in Figure 3.5. Following this step, the electric current injection value will also be defined and integrated into the line created at the center of the PV module.
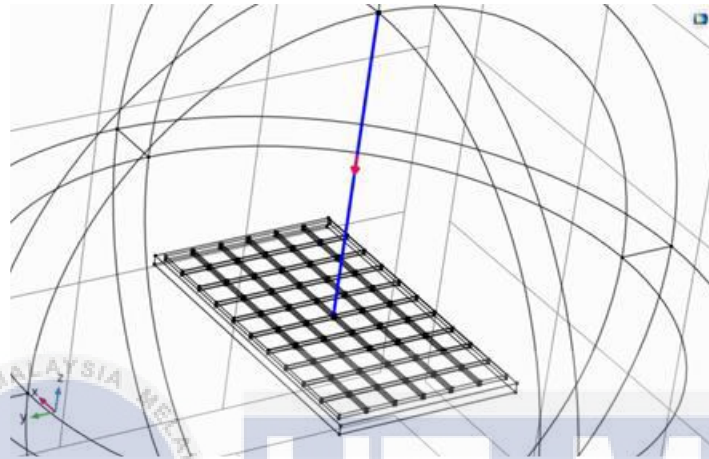
Figure 3.5 Line of Electric Current Injection

As depicted in Figure 3.5, a line representing electric current injection has been established. This line will be subjected to two proposed conditions: normal and lightning. Accordingly, a current of 8A has been selected for the normal condition [53], whereas for the lightning condition, it has been specified with a total current of 30kA [54]. These values have been organized in Table 3.5, and it's crucial to alternate between these conditions during the simulation.

Condition	Electric Current Injection (A)
Normal	8
Lightning	30,000

Table 3.4 Electric Current Injection of Normal and Lightning Condition

3.6 Simulation Test

A simulation test involves assessing a model or system virtually through computer-based simulations rather than conducting physical experiments in the real world. This process entails generating a digital representation of the system, typically utilizing specialized software, to replicate its behavior and forecast its performance across different conditions. In this project, the model under examination is the PV module that has been developed, and it will undergo simulation using the COMSOL Multiphysics software.

3.6.1 Magnetic Field and Magnetic Flux Density under Normal and Lightning Condition

The model employed in this section employs polycrystalline silicon as the material for the solar cells and incorporates current injection at the midpoint of the PV module. The model is depicted in Figure 3.7 and will undergo testing alternately under normal and lightning conditions.

After configuring the current injection value to 8A [53], the model enters a normal condition and is prepared for simulation. During the simulation, a magnetic distribution will be generated, comprising magnetic field and magnetic flux density values. These values will be extracted by transferring data from COMSOL to Excel

37

for each point on the PV module. Additionally, a sorting phase will be conducted, limiting the values from minimum to maximum along the positive-y direction.
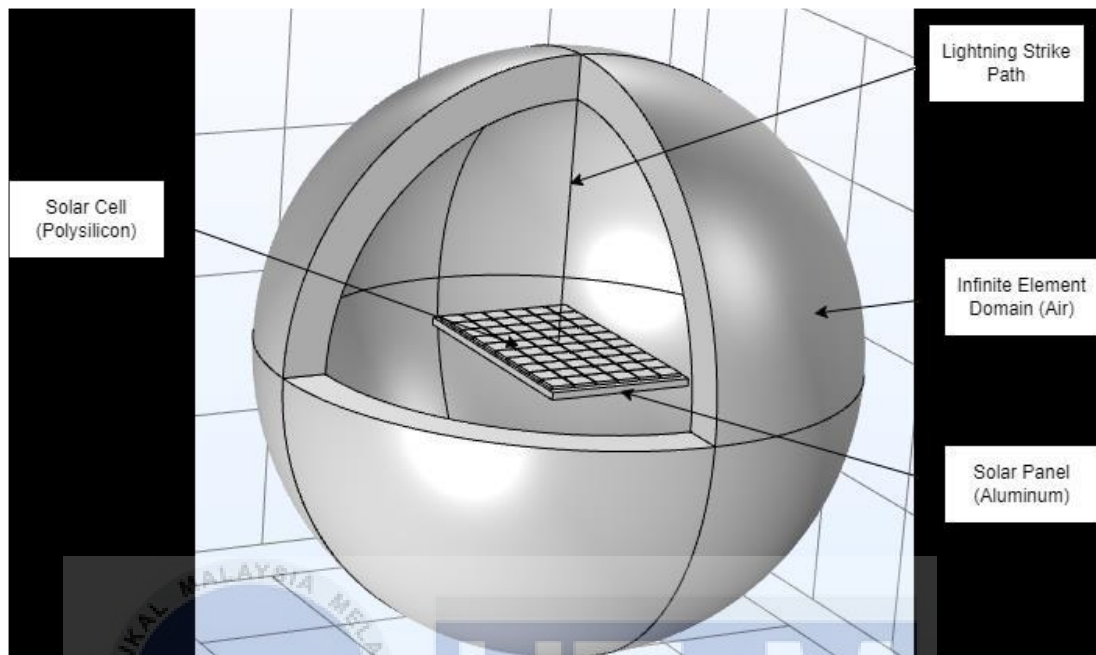
Figure 3.6 PV Module of Polysilicon and Middle Current Injection

Following this, the values will be organized into a table and compared to the standard limits outlined in BS EN 61000-4-9 from Table 3.1. This comparison will ascertain whether the simulated results fall within the permissible range. Similarly, the model will undergo simulation again, but this time utilizing 30kA as the new current injection for the lightning condition [54]. It's crucial to compare the normal and lightning conditions to identify which one yields a higher output of magnetic field and magnetic flux density.

38

3.6.2 Effect on Different Injection Point of Electric Current Toward Magnetic Field and Magnetic Flux Density

In this section, the simulation follows the same steps outlined in Section 3.6.1. However, there are two injection points for electric current that will be analyzed: the middle point and the corner point of the PV module. This is illustrated in Figure 3.7 and Figure 3.8. Both models will utilize Polysilicon as the material for the solar cells and will be tested under normal and lightning conditions.
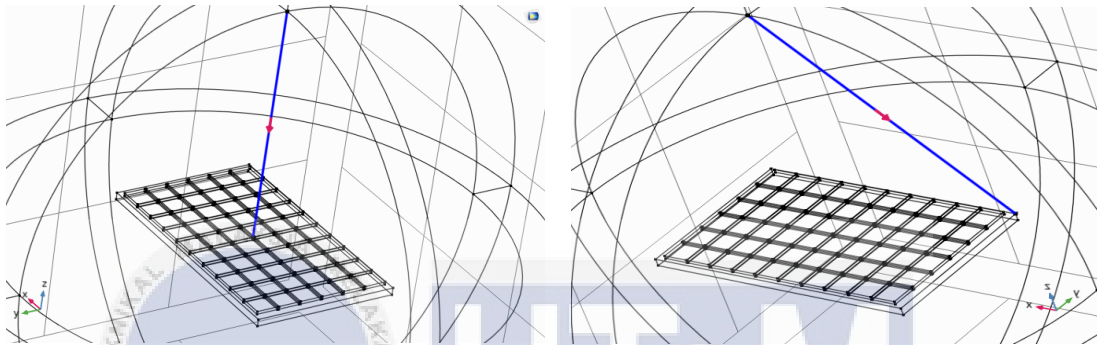
Figure 3.8 Middle Injection Point   Figure 3.7 Corner Injection Point

Data from both points will be organized into tables and compared to the standard limits specified in BS EN 61000-4-9 from Table 3.1. This analysis will identify which injection point generates magnetic interference within the acceptable limits. Additionally, a comparison between the magnetic interference of the middle injection point and the corner injection point will be conducted to determine which one yields a higher output of magnetic field and magnetic flux density.

3.6.3 Effect on Different Solar Cell Material Toward Magnetic Field and Magnetic Flux Density

For this scenario, the focus will be on simulating the middle injection point of the PV module. Additionally, the material for the solar cells will be modified, replacing

Polysilicon with Monocrystalline Silicon and Thin-Film (Gallium Arsenide), as depicted in Figure 3.9. The adjustment in materials primarily involves the electrical properties of electrical conductivity, relative permeability, and relative permittivity. Consequently, data from Table 3.4 were utilized to establish the values for each type of material.
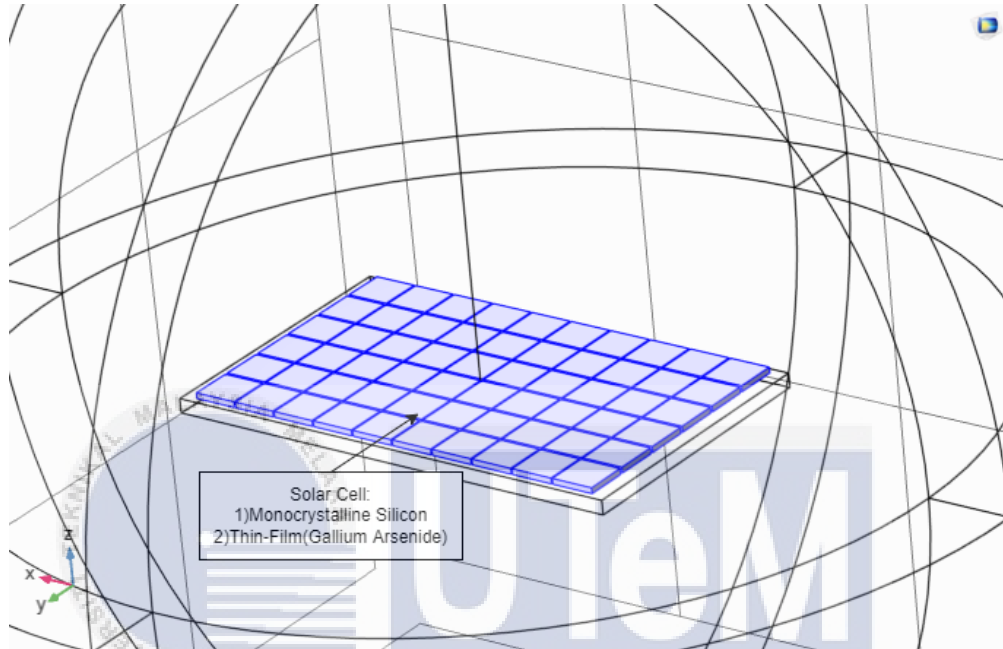
Figure 3.9 Solar Cell Part in PV Module

Upon updating the input of solar cell properties to Monocrystalline Silicon, the model will undergo simulation under both normal and lightning conditions. This will generate a magnetic distribution comprising magnetic field and magnetic flux density. Subsequently, the data will be sorted, tabulated, and compared with the standard limits specified in BS EN 61000-4-9 from Table 3.1.

Subsequently, the model will be simulated again under both conditions, but with the input now changed to the new material, Thin-Film (Gallium Arsenide). The resulting values will be tabulated and assessed against the same standard limits as for Monocrystalline Silicon. Finally, comparisons of Magnetic Field and Magnetic Flux Density between Polycrystalline Silicon and the other solar cell materials involved in this project will be made. This analysis will aid in determining which materials exhibit lower induced current due to external magnetic fields and magnetic flux density. Additionally, the efficiency of solar production for each material will be examined.

CHAPTER 4

RESULTS AND DISCUSSIONS

4.1 Introduction

This chapter will present the outcomes and examination derived from the methodology proposed in Chapter 3. It encompasses the PV module design and assesses the impact of magnetic field and magnetic flux density interference under both normal and lightning conditions. Furthermore, it incorporates an evaluation of the influences of various lightning strike points and solar cell materials on magnetic field and flux density. This analysis will also be juxtaposed with the standard limits outlined in the BSI Standard of Electromagnetic Compatibility (EMC) -BS EN 61000-4-9.

4.2 Design of a PV Module using Comsol Multiphysics Software
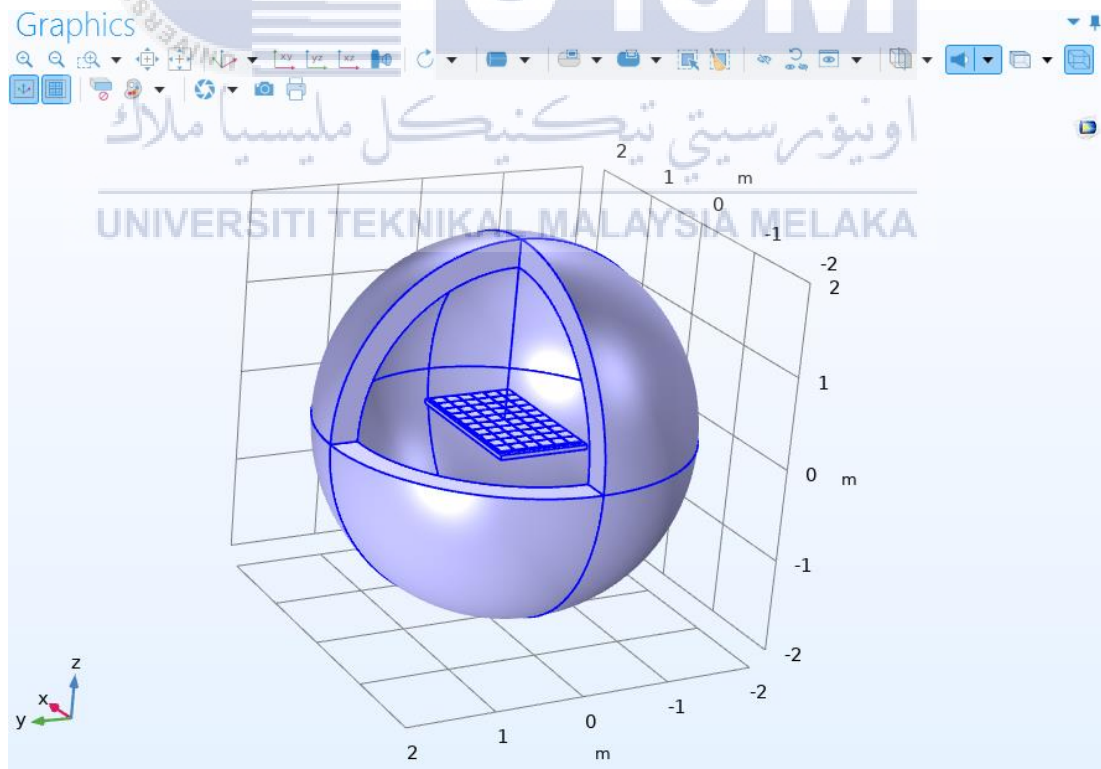
Figure 4.1 3D Model of PV Module

41

The 3D model of PV modules depicted in Figure 4.1 illustrates the configuration created with a specified circle size of air domain utilizing COMSOL Multiphysics software. This model comprises an aluminum frame, solar cell, air domain, and a line for current injection. The dimensions for each primary component are determined according to Table 3.2 and Table 3.3.

Within this model, three elements will be varied for analysis in alignment with the objectives: the location of electric current injection, the value of electric current injection, and the solar cell material. Regarding the location of electric current injection, both the center and corner of the PV module were selected. These locations are depicted in Figure 4.2 and Figure 4.3.
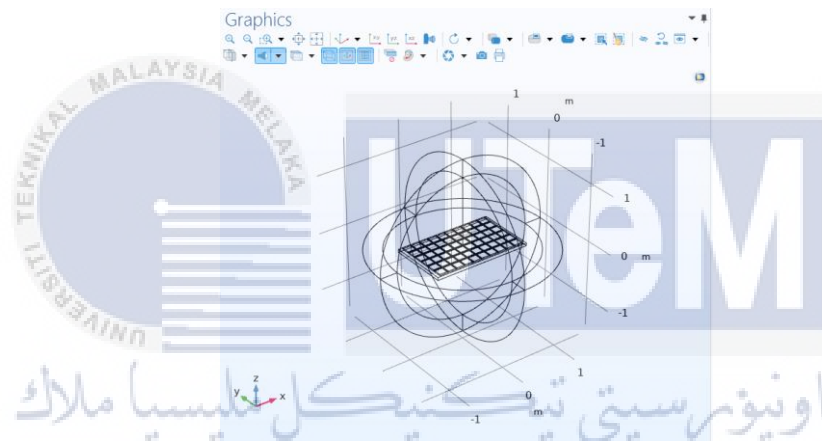
Figure 4.2 Middle Strike Injection Point
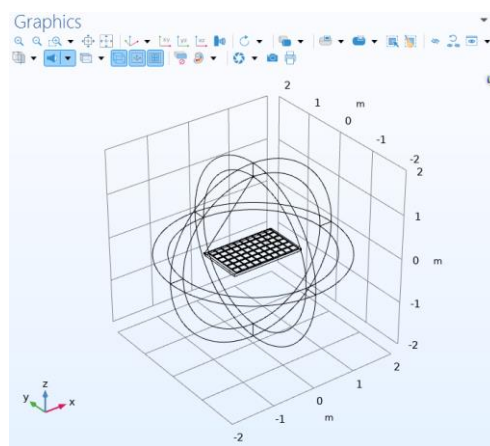
Figure 4.3 Corner Strike Injection Point

The current settings for these locations have been established to account for two conditions: lightning and normal operations, with predetermined values listed in Table 3.5. Meanwhile, analysis includes three material types: Polycrystalline Silicon, Monocrystalline Silicon, and Thin-Film (Gallium Arsenide). Adjustments for different materials primarily consider electrical properties such as relative permeability, relative permittivity, and electrical conductivity. The values for each material type are determined based on data provided in Table 3.4.

4.3 Interference of Magnetic Field and Magnetic Flux Density Under Normal and Lightning Condition

In this section, the model employed is designed for electric current injection at the midpoint of the PV module, utilizing Polycrystalline Silicon as the material for the solar cells. The model was executed under two scenarios: lightning and normal conditions, applying the electric current injection values provided in Table 3.5.
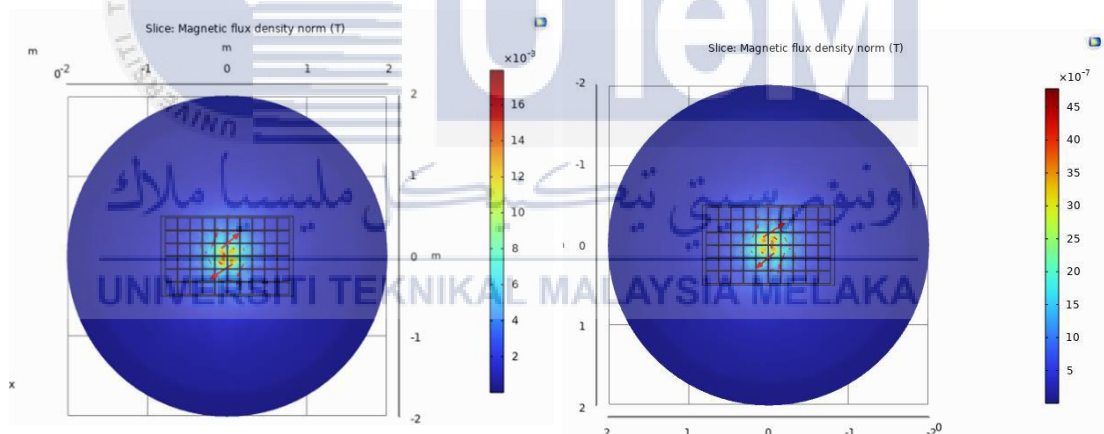
Figure 4.5 Lightning Magnetic Flux Density Distribution

Figure 4.4 Normal Magnetic Flux Density Distribution

43
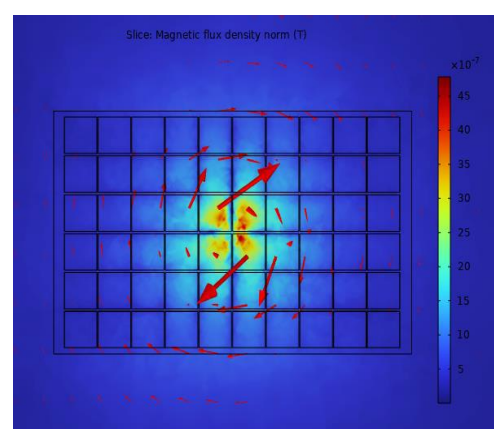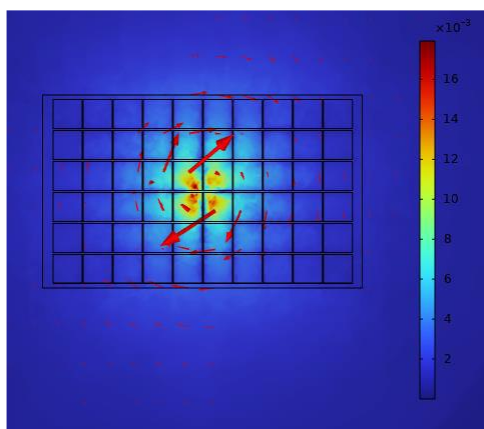
According to Figures 4.4 and 4.5, the distribution of magnetic flux density starts from the lowest value and gradually increases to the highest value. This distribution pattern remains consistent across both lightning and normal conditions. The blue zone indicates a low magnetic flux density, primarily due to its distance from the injection point, while values escalate towards the injection point. Notably, the highest magnetic flux density is observed near the injection point, represented as the red zone. Further examination of these values can be found in the tables below.

| Condition | Magnetic Field (A/m) | | | | | BS EN 61000-4-9 Standard Limit (A/m) | Percentage differences of Average Magnetic Field & Standard Limit (%) | Magnetic Field Level |
	Maximum	Coordinate	Minimum	Coordinate	Average			
Lightning	53030.99	X= -0.03534971 Y= -0.005 Z= 0.045	9.4630	X= -0.03534971 Y= 0.165 Z= 0.025	2769.78	1000	176.98	Exceed Limit
Normal	14.141		0.002523		0.73861	1000	-99.93	Within Limit

Table 4.1 Magnetic Field in Lightning and Normal Condition(Middle Point)

In the lightning condition, the maximum and minimum values of magnetic field produced are 53030.99 A/m and 9.4630 A/m, respectively. The calculated average value is 2769.78 A/m, which is approximately 176.98% higher than the standard limit. Conversely, during normal conditions, the magnetic field reaches a maximum of 14.141 A/m and a minimum of 0.002523 A/m. The calculated average value is 0.73861 A/m, which falls within the standard limit.

| Condition | Magnetic Flux Density (T) | | | | | BS EN 61000-4-9 Standard Limit (µT) | Percentage differences of Average Magnetic Flux & Standard Limit (%) | Magnetic Flux Density Level |
	Maximum	Coordinate	Minimum	Coordinate	Average			
Lightning	0.066635	X= -0.03534971 Y= -0.005 Z= 0.045	1.19E-5	X= -0.03534971 Y= 0.165 Z= 0.025	0.003480	1260	176.19	Exceed Limit
Normal	1.78E-05		3.17E-09		9.35E-07	1260	-99.93	Within Limit

Table 4.2 Magnetic Flux Density in Lightning and Normal Condition(Middle Point)

In the lightning condition, the magnetic flux density reaches 0.066635 T at its maximum and 1.19e-5 T at its minimum. The calculated average value is 0.003480 T, which exceeds the standard limit by approximately 176.19%. Conversely, during normal conditions, the magnetic flux density ranges from 1.78e-5 T (maximum) to 3.17e-9 T (minimum). The calculated average value is 9.35e-7 T, which falls within the standard limit.

Condition	Magnetic Field (A/m)		Magnetic Flux Density (T)	
	Average	Difference of Lightning and Normal Condition (%)	Average	Difference of Lightning and Normal Condition (%)
Lightning	2769.78	99.97	0.003480	99.97
Normal	0.73861		9.35E-07	

Table 4.3 Comparison between Lightning and Normal Condition(Middle Point)

It's evident that during lightning conditions, both the magnetic field and magnetic flux density are approximately 99.97% larger compared to normal conditions. Consequently, this substantial increase in induced current poses a significant risk of severe damage to the PV module.

4.4 Effect of Different Injection Point of Electric Current Toward Magnetic Field and Magnetic Flux Density.

This section involves utilizing the model with injection points at both the middle and corner of the PV module, employing Polycrystalline Silicon as the material for solar cells. The model undergoes simulation under two conditions: lightning and normal, utilizing the electric current injection values specified in Table 3.5.
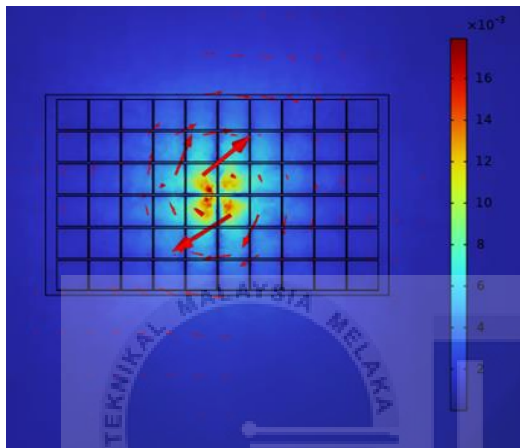
Figure 4.9 Lightning Magnetic Flux Density Distribution(Middle)
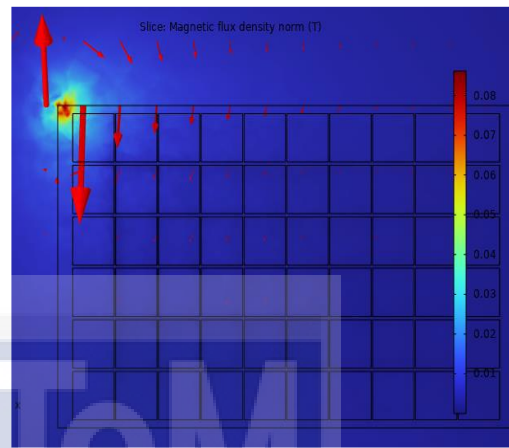
Figure 4.8 Lightning Magnetic Flux Density Distribution(Corner)
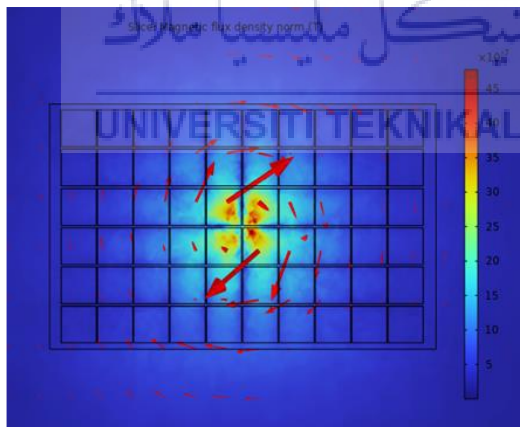
Figure 4.7 Normal Magnetic Flux Density Distribution(Middle)
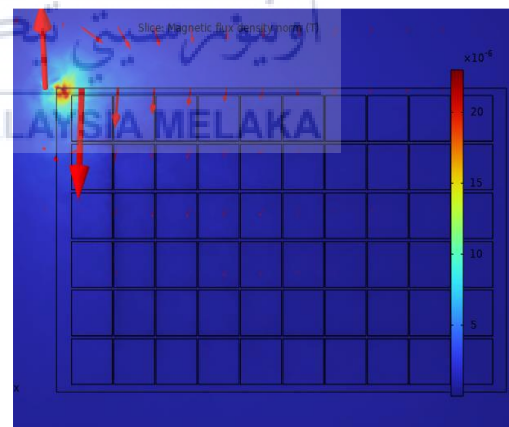
Figure 4.6 Normal Magnetic Flux Density Distribution(Corner)

According to the figure above, the magnetic flux density distribution ranges from the lowest to the highest value. This distribution pattern remains consistent across both lightning and normal conditions. The blue zone exhibits a low magnetic flux density, attributed to its distance from the injection point, with values increasing towards the injection point. Notably, the highest magnetic flux density is observed near the injection point, represented as the red zone. While the values for the middle strike of the PV module were recorded in Section 4.3, the data for the corner strike can be examined in the tables below.

Condition	Magnetic Field (A/m)					BS EN 61000-4-9 Standard Limit (A/m)	Percentage differences of Average Magnetic Field & Standard Limit (%)	Magnetic Field Level
	Maximum	Coordinate	Minimum	Coordinate	Average			
Lightning	18278.27	X= -0.825 Y= 0.456340389 Z= 0.025	7.6306	X= 0.662356381	925.14	1000	-7.49	Within Limit
Normal	4.8742		0.002034	Y= -0.338801826 Z= -0.025	0.24670	1000	-99.98	Within Limit

Table 4.2 Magnetic Field of Lightning and Normal Condition(Corner Point)

In the lightning condition, the magnetic field reaches a maximum of 18278.27 A/m and a minimum of 7.6306 A/m. The calculated average value is 925.14 A/m, which is approximately 7.49% lower than the standard limit. Conversely, during normal conditions, the magnetic field ranges from 4.8742 A/m (maximum) to 0.002034 A/m (minimum). The calculated average value is 0.2467 A/m, which falls within the standard limit.

Condition	Magnetic Flux Density (T)					BS EN 61000-4-9 Standard Limit (μT)	Percentage differences of Average Magnetic Flux & Standard Limit (%)	Magnetic Flux Density Level
	Maximum	Coordinate	Minimum	Coordinate	Average			
Lightning	0.022969	X= -0.825 Y= 0.456340389 Z= 0.025	9.59E-06	X= 0.662356381 Y= -0.338801826 Z= -0.025	0.001112	1260	-11.75	Within Limit
Normal	6.13E-06		2.56E-09		2.97E-07	1260	-99.98	Within Limit

Table 4.3 Magnetic Flux Density of Lightning and Normal Condition(Corner Point)

In the lightning condition, the magnetic flux density reaches 0.022969 T at its maximum and 9.59e-6 T at its minimum. The calculated average value is 0.001112 T, which is approximately 11.75% lower than the standard limit. Conversely, during normal conditions, the magnetic flux density ranges from 6.13e-6 T (maximum) to 2.56e-9 T (minimum). The calculated average value is 2.97e-7 T, which falls within the standard limit.

Injection Point	Lightning Magnetic Field (A/m)		Normal Magnetic Field (A/m)	
	Average	Difference of Middle and Corner Strike (%)	Average	Difference of Middle and Corner Strike (%)
Middle Strike	2769.78	66.60	0.73861	66.60
Corner Strike	925.14		0.24670	

Table 4.4 Comparison of Magnetic Field between Middle and Corner of Injection Point

It's notable that during both lightning and normal conditions, the magnetic field generated at the corner strike point is approximately 66.6% smaller compared to that at the middle strike point.

Injection Point	Lightning Magnetic Flux Density (T)		Normal Magnetic Flux Density (T)	
	Average	Difference of Middle and Corner Strike (%)	Average	Difference of Middle and Corner Strike (%)
Middle Strike	0.003480	68.05	9.35E-07	68.24
Corner Strike	0.001112		2.97E-07	

Table 4.5 Comparison of Magnetic Flux Density between Middle and Corner of Injection Point

Observations reveal that during lightning conditions, the magnetic flux density generated at the corner strike point is approximately 68.05% smaller than that at the middle strike point. Similarly, in normal conditions, it is approximately 68.24% smaller than at the middle strike point. Consequently, the corner strike injection point induces lower current, resulting in less damage to the PV module compared to the middle strike injection point.
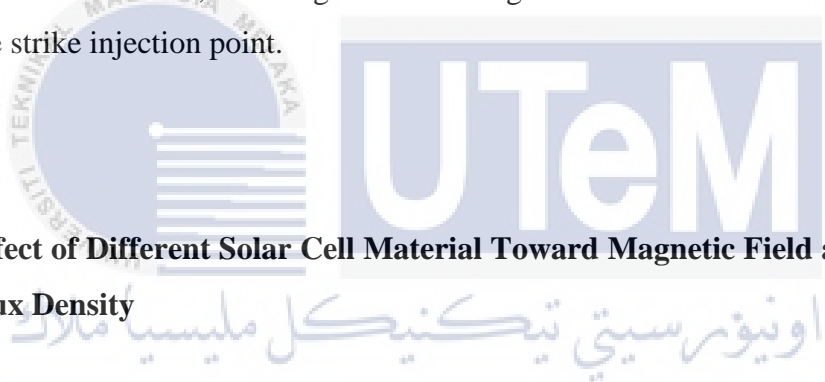
4.5 Effect of Different Solar Cell Material Toward Magnetic Field and Magnetic Flux Density

In this part, the model that was used is restriced to the injection point in middle strike of the PV module and was run in lightning and normal condition. In this case, the major difference is by changing solar cell material from Polycrystalline Silicon to Monocrystalline Silicon and Thin-Film (Gallium Arsenide). The adjustment in terms of material is more focused on electrical properties which are relative permeability, relative permittivity, and electrical conductivity. The value for each type of material was set using data in Table 3.4.
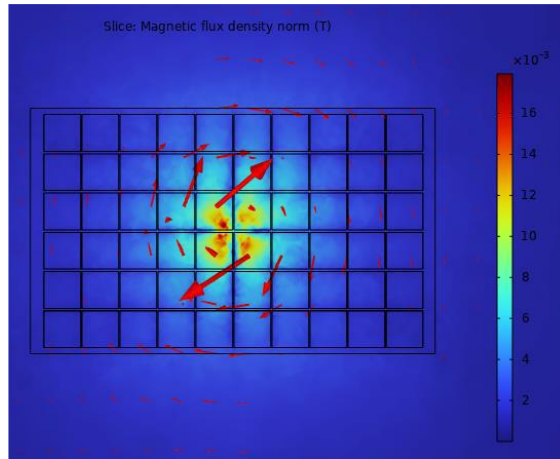
Figure 4.10 Magnetic Flux Density Distribution of Monocrystalline Silicon and
Thin-Film (Gallium Arsenide)

As depicted in Figure 4.10, the distribution of magnetic flux density ranges from the
lowest to the highest value. This distribution pattern for Monocrystalline Silicon and
Thin-Film Silicon (Gallium Arsenide) is identical to that of Polycrystalline Silicon.
The blue zone, located farther from the injection point, exhibits a lower magnetic flux
density, with values increasing towards the injection point.

Furthermore, it was observed that the red zone, representing the injection site,
displayed the highest magnetic flux density. While the values for Polycrystalline
Silicon were recorded in Section 4.3, the data for the other solar cell materials can be
examined in the tables below.

- Monocrstalline Silicon

Condition	Magnetic Field (A/m)					BS EN 61000-4-9 Standard Limit (A/m)	Percentage differences of Average Magnetic Field & Standard Limit (%)	Magnetic Field Level
	Maximum	Coordinate	Minimum	Coordinate	Average			
Lightning	53019.85	X= -0.03534971	8.9041	X= -0.03534971	2769.61	1000	176.96	Exceed Limit
Normal	14.139	Y= -0.005 Z= 0.045	0.002374	Y= 0.165 Z= 0.025	0.73856	1000	-99.93	Within Limit

Table 4.6 Magnetic Field of Monocrystalline Silicon

50

During lightning conditions, the magnetic field reaches a maximum of 53019.85 A/m and a minimum of 8.9041 A/m. The calculated average value is 2769.61 A/m, representing approximately 176.96% above the standard limit. In contrast, under normal circumstances, the magnetic field ranges from a maximum of 14.139 A/m to a minimum of 0.002374 A/m. The calculated average value, 0.73856 A/m, falls within the acceptable range.

| Condition | Magnetic Flux Density (T) | | | | | BS EN 61000-4-9 Standard Limit (µT) | Percentage differences of Average Magnetic Flux & Standard Limit (%) | Magnetic Flux Density Level |
	Maximum	Coordinate	Minimum	Coordinate	Average			
Lightning	0.066574	X= -0.03534971 Y= -0.005 Z= 0.045	1.12E-05	X= -0.03534971 Y= 0.165 Z= 0.025	0.003478	1260	176.03	Exceed Limit
Normal	1.775E-05		2.98E-09		9.275E-07	1260	-99.93	Within Limit

Table 4.7 Magnetic Flux Density of Monocrystalline Silicon

During lightning conditions, the magnetic flux density reaches a maximum of 0.066574 T and a minimum of 1.12e-5 T. The calculated average value is 0.003478 T, representing approximately 176.03% above the standard limit. Meanwhile, under normal circumstances, the magnetic flux density ranges from a high of 1.775e-5 T to a low of 2.98e-9 T. The average value calculated, 9.275e-7 A/m, falls within the acceptable range.

51

- Thin-Film Silicon (Gallium Arsenide)

Condition	Magnetic Field (A/m)					BS EN 61000-4-9 Standard Limit (A/m)	Percentage differences of Average Magnetic Field & Standard Limit (%)	Magnetic Field Level
	Maximum	Coordinate	Minimum	Coordinate	Average			
Lightning	53032.09	X= -0.03534971	9.5186	X= -0.03534971	2769.80	1000	176.99	Exceed Limit
Normal	14.142	Y= -0.005 Z= 0.045	0.002538	Y= 0.165 Z= 0.025	0.73862	1000	99.93	Within Limit

Table 4.8 Magnetic Field of Thin-Film Silicon (Gallium Arsenide)

During lightning conditions, the maximum magnetic field strength reaches 53032.09 A/m, while the minimum strength is 9.5186 A/m. The average value, estimated at 2769.80 A/m, exceeds the permitted maximum by approximately 176.99%. Conversely, under normal conditions, the magnetic field ranges from a high of 14.142 A/m to a low of 0.002538 A/m. The computed average value of 0.73862 A/m falls within the allowed range.

Condition	Magnetic Flux Density (T)					BS EN 61000-4-9 Standard Limit (µT)	Percentage differences of Average Magnetic Flux & Standard Limit (%)	Magnetic Flux Density Level
	Maximum	Coordinate	Minimum	Coordinate	Average			
Lightning	0.066642	X= -0.03534971	1.20E-05	X= -0.03534971	0.003482	1260	176.35	Exceed Limit
Normal	1.79E-05	Y= -0.005 Z= 0.045	3.19E-09	Y= 0.165 Z= 0.025	9.28E-07	1260	-99.93	Within Limit

Table 4.9 Magnetic Flux Density of Thin-Film Silicon (Gallium Arsenide)

In a lightning scenario, the maximum and minimum magnetic flux densities generated are 0.066642 T and 1.20e-5 T, respectively. The average value, approximately 176.35% higher than the standard limit, was calculated to be 0.003478 T. Under normal conditions, the magnetic flux density ranges from a maximum of 1.79e-5 T to a minimum of 3.19e-9 T. The determined average value, 9.28e-7 A/m, falls within the allowed range.

Solar Cell Material	Lightning Magnetic Field (A/m)		Normal Magnetic Field (A/m)	
	Average	Difference of Polycrystalline Silicon and Selected Material	Average	Difference of Polycrystalline Silicon and Selected Material
Polycrystalline Silicon	2769.78	-	0.73861	-
Monocrystalline Silicon	2769.61	0.17	0.73856	0.00005
Thin-Film Silicon (Gallium Arsenide)	2769.80	-0.02	0.73862	-0.00001

Table 4.10 Comparison of Solar Cell Materials in Magnetic Field

It is noted that when utilizing Monocrystalline Silicon, the magnetic field produced is slightly lower than that of Polycrystalline Silicon, approximately by 0.17 A/m during lightning and 0.00005 A/m during normal conditions. Conversely, for Gallium Arsenide, it yields a magnetic field slightly higher than Polycrystalline Silicon, approximately by 0.02 A/m during lightning and 0.00001 A/m during normal conditions.

Solar Cell Material	Lightning Magnetic Flux Density (T)		Normal Magnetic Flux Density (T)	
	Average	Difference of Polycrystalline Silicon and Selected Material	Average	Difference of Polycrystalline Silicon and Selected Material
Polycrystalline Silicon	0.003480	-	9.35E-07	-
Monocrystalline Silicon	0.003478	2e-6	9.275E-07	0.075e-7
Thin-Film Silicon (Gallium Arsenide)	0.003482	-2e-6	9.28E-07	0.007e-7

Table 4.11 Comparison of Solar Cell Materials in Magnetic Flux Density

It has been observed that the magnetic flux density generated by Monocrystalline Silicon is slightly lower than that of Polycrystalline Silicon, approximately 2e-6 T under lightning conditions and 0.075e-7 T during normal conditions. In contrast, the magnetic flux density produced by Gallium Arsenide is slightly higher than that of

Polycrystalline Silicon, approximately -2e-6 T during lightning and 0.007e-7 T during normal conditions.

Therefore, it is concluded that Monocrystalline Silicon produces the lowest magnetic field and magnetic flux density, albeit by a small margin compared to other materials. This indicates that the material possesses high resistivity while exhibiting lower induced current, potentially enhancing the efficiency of solar energy production.

CHAPTER 5

CONCLUSION AND RECOMMENDATIONS

5.1 Conclusion

In summary, lightning significantly contributes to the failure of PV systems. The extent of damage to PV modules and associated equipment correlates with the strength of the magnetic field generated by lightning strikes. This, in turn, disrupts the flow of induced current, leading to decreased efficiency. The primary goal of creating a 3D model of the PV module with a specified air domain size using COMSOL Multiphysics software has been successfully accomplished. Regarding the second objective, it has been established that during lightning conditions, the magnetic field and flux density are approximately 99.97% greater compared to normal conditions. Consequently, the heightened induced current poses a severe threat to the integrity of the PV module.

In case 1, the observation reveals that during both lightning and normal conditions, the magnetic field generated at the corner strike point is 66.6% smaller than that at the middle strike point. Consequently, the corner strike injection point experiences lower induced current, resulting in less damage to the PV module compared to the middle strike injection point. Moving on to case 2, it has been established that Monocrystalline Silicon exhibits the lowest magnetic field and magnetic flux density among the tested materials, albeit by a narrow margin. This indicates that the material possesses high resistivity, leading to reduced induced current, ultimately enhancing the efficiency of solar energy production.

5.2 Future Works

Based on the research conducted and the findings outlined in this report, a prospective avenue for future exploration becomes evident: delving deeper into the impact of air domain size on magnetic field and magnetic flux density.

REFERENCES

1. Becquerel, A.E. Memoire Sur Les Effects d'Electriques Produits Sous l'Influence Des Rayons Solaires. *Comptes Rendus De L'academie Des Sci.* **1839**, *9*, 561–567. (accessed on 27 October 2022).

2. Fritts, C.E. On a New Form of Selenium Cell, and Some Electrical Discoveries Made by Its Use. *Am. J. Sci.* **1883**, *s3-26*, 465–472.

3. Weston, E. Apparatus for Utilizing Solar Radiant Energy. U.S. Patent 389124A, 4 September 1888.

4. Oh, R.S. Light-Sensitive Electric Device. U.S. Patent 2402662A, 27 May 1941.

5. Ohl, R. Light-Sensitive Electric Device Including Silicon. U.S. Patent 2, 443,542, 15 June 1948.

6. Neamen, D.A. *Semiconductor Physics and Devices: Basic Principles*; McGraw-Hill: New York, NY, USA, 2012.

7. Smith, R.P.; Hwang, A.A.-C.; Beetz, T.; Helgren, E. Introduction to semiconductor processing: Fabrication and characterization of p-n junction silicon solar cells. *Am. J. Phys.* **2018**, *86*, 740–746.

8. Seeger, K. *Semiconductor Physics*; Springer Science & Business: Berlin/Heidelberg, Germany, 2013.

9. Smets, A.H.M.; Jager, K.; Isabella, O.; van Swaaij, R.A.; Zeman, M. Solar Cell Parameters and Equivalent Circuit. *Sol. Energy Phys. Eng. Photovolt. Convers. Technol. Syst.* **2016**, 113–121.

10. Sze, S.M.; Ng, K.K. Photodetectors and Solar Cells. In *Physics of Semiconductor Devices*; John Wiley & Sons, Inc.: Hoboken, NJ, USA, 2006; pp. 663–742.

11. Sharma, D.; Mehra, R.; Raj, B. Comparative analysis of photovoltaic technologies for high efficiency solar cell design. *Superlattices Microstruct.* **2021**, *153*, 106861.

12. Zhang, C.; Honsberg, C.; Faleev, N.; Goodnick, S. *High Efficiency GaAs-Based Solar Cells Simulation and Fabrication*; Arizona State University: Phoenix, AZ, USA, 2014.

13. Radziemska, E. Thermal performance of Si and GaAs based solar cells and modules: A review. *Prog. Energy Combust. Sci.* **2003**, *29*, 407–424.

14. Floyd, T.L. *Electronic Devices*, 9th ed.; Pearson: London, UK, 2011.

15. Arefeen, S.; Dallas, T. Low-cost racking for solar photovoltaic systems with renewable tensegrity structures. *Sol. Energy* **2021**, *224*, 798–807.

16. Saravanan, S.; Krishna Teja, T.; Dubey, R.S.; Kalainathan, S. Design and analysis of GaAs thin film solar cell using an efficient light trapping bottom structure. *Mater. Today Proc.* **2016**, *3*, 2463–2467.

17. Dzimano, G. *Modeling of Photovoltaic Systems*; Ohio State University: Columbus, OH, USA, 2008.

18. Hamaguchi, C. *Basic Semiconductor Physics*; Springer-Verlag: Berlin, Germany, 2010; Volume 9.

19. Bhuvaneswari G, Annamalai R Development of a solar cell model in MATLAB for PV based generation system. Annual IEEE India Conference; 2011 Dec 16-18; Hyderabad: IEEE; 2011. p. 1-5.

20. Kane A, Verma V Characterization of PV cell-environmental factors consideration. International Conference on Power, Energy and Control; 2013 Feb 6-8; Sri Rangalatchum Dindigul: IEEE; 2013. p. 26-29.

21. Tiwari GN, Dubey S. Fundamentals of photovoltaic modules and their applications. UK: Royal Society of Chemistry; 2010.

22. Shah A, Torres P, Tscharner R, Wyrsch N, Keppner H. Photovoltaic technology: the case for thin-film solar cells. Science 1999;8(285):692–8.

23. Green MA. Solar cells: operating principles, technology, and system applications. Englewood Cliffs, NJ: Prentice-Hall, Inc; 1982.

24. Falk F, Andra G. Crystalline silicon thin film solar cells. INTECH Open Access Publisher; 2011.

25. Pinheiro WA, Falcão VD, Cruz LR dO, Ferreira CL. Comparative study of CdTe sources used for deposition of CdTe thin films by close spaced sublimation technique. Mater Res 2006;3(9):47–9.

26. Sonnenenergie DGF. Planning and installing photovoltaic systems: a guide for installers, architects and engineers, 2nd ed. Earthscan; 2008.

27. Saga T. Advances in crystalline silicon solar cell technology for industrial mass production. NPG Asia Mater 2010;7(2):96–102.

28.   Bruton T. General trends about photovoltaics based on crystalline silicon. Sol Energy Mater Sol Cells 2002;8(72):3–10.

29.   Parida B, Iniyan S, Goic R. A review of solar photovoltaic technologies. Renew Sustain Energy Rev 2011;12(15):1625–36.

30.   Zhao Y. Fault analysis in solar photovoltaic arrays [dissertation]. Northeastern University; 2010.

31.   Kadir M, Misbah N, Gomes C, Jasni J, Ahmad WW, Hassan M Recent statistics on lightning fatalities in Malaysia. International Conference on Lightning Protection; 2012 Sep 2-7; Vienna: IEEE; 2012. p. 1-5.

32.   Uman MA. The lightning discharge. New York: Dover Publications, Inc; 2001.

33.   Srinivasan K, Gu J. Lightning as atmospheric electricity. Canadian Conference on Electrical and Computer Engineering; 2006 May 7-10; Ottawa, Ont: IEEE; 2006. p. 2258–2261.

34.   Cooray V. Lightning protection. Inst Eng Technol 2010.

35.   Cooray V. The lightning flash. Inst Eng Technol 2003.

36.   Guideline on Lightning Protection for Photovoltaic (PV) Systems. Sustainable Energy Development Authority Malaysia; 2016.

37.   Rakov VA, Uman MA. Lightning: physics and effects. Cambridge University Press; 2003.

38.   Bouquegneau C Lightning density based on lightning location systems. International Conference on Lightning Protection; 2014 Oct 11-18; Shanghai: IEEE; 2014. p. 1947–1951.

39.   Damage Statistic for Solar PV due to lightning, ⟨https://www.dehn-international. com⟩ [accessed 13 May 2016]; 2016

40.   V. A. Rakov, "Lightning Discharge and Fundamentals of Lightning Protection," *Journal of Lightning Research*, vol. 4, no. 1, pp. 3–11, Jun. 2012, doi: 10.2174/1652803401204010003.

41.   C. A. Christodoulou, L. Ekonomou, I. F. Gonos, and N. P. Papanikolaou, "Lightning protection of PV systems," *Energy Systems*, vol. 7, no. 3, pp. 469–482, Aug. 2016, doi: 10.1007/s12667-015-0176-2.

42.   A. I. Tarmizi, R. H. Ramlee, and M. D. Rotaru, "Electromagnetic Compatibility Analysis of Substation Environment using Finite Difference Method," *International Journal of Innovative Technology and Exploring Engineering*, vol. 8, no. 12S2, pp. 521–527, Dec. 2019, doi: 10.35940/ijitee.l1097.10812s219.

43. R. Araneo, S. Lammens, M. Grossi, and S. Bertone, "EMC issues in high-power grid-connected photovoltaic plants," *IEEE Trans Electromagn Compat*, vol. 51, no. 3 PART 2, pp. 639–648, 2009, doi: 10.1109/TEMC.2009.2026055.

44. N. H. Zaini *et al.*, "Lightning surge analysis on a large scale grid-connected solar photovoltaic system," *Energies (Basel)*, vol. 10, no. 12, Dec. 2017, doi: 10.3390/en10122149.

45. K. M. Coetzer, P. Gideon Wiid, and A. J. Rix, "Investigating Lightning Induced Currents in Photovoltaic Modules," in *EMC Europe 2019 - 2019 International Symposium on Electromagnetic Compatibility*, Institute of Electrical and Electronics Engineers Inc., Sep. 2019, pp. 261–266. doi: 10.1109/EMCEurope.2019.8871890.

46. IEC Corporation, *BS 61000-4-9 BRITISH STANDARD Electromagnetic compatibility (EMC)-Part 4-9: Testing and measurement techniques-Pulse Impulse magnetic field immunity test INTERNATIONAL ELECTROTECHNICAL COMMISSION*, 2.0. 2016.

47. N. H. Zaini *et al.*, "On the effect of lightning on a solar photovoltaic system," in *2016 33rd International Conference on Lightning Protection, ICLP 2016*, Institute of Electrical and Electronics Engineers Inc., Dec. 2016. doi: 10.1109/ICLP.2016.7791421.

48. S. Sugianto, "Comparative Analysis of Solar Cell Efficiency between Monocrystalline and Polycrystalline," *INTEK: Jurnal Penelitian*, vol. 7, no. 2, p. 92, Dec. 2020, doi: 10.31963/intek.v7i2.2625.

49. US Department of Energy, "Solar Panel Size and Weight: How Big Are Solar Panels? | EnergySage," 2009. https://news.energysage.com/average-solar-panel-size-weight/ (accessed Jul. 07, 2023).

50. US Department of Energy, "Solar Panel Size and Weight: How Big Are Solar Panels? | EnergySage," 2009. https://news.energysage.com/average-solar-panel-size-weight/ (accessed Jul. 07, 2023).

51. T. C. Edwards and M. B. Steer, "Appendix B: Material Properties," in *Foundations for Microstrip Circuit Design*, John Wiley & Sons, Ltd, 2016, pp. 635–642. doi: 10.1002/9781118936160.app2.

52. W. Kappel, G. Alecu, V. Tsakiris, W. Kappel, and G. Alecu, "Solid state diffusion welding of Cu-Fe/Al/Ag and Al-Ni dissimilar metals," *Article in Journal of*

Optoelectronics and Advanced Materials, vol. 13, no. 9, pp. 1176–1180, 2011, doi: 10.13140/2.1.1684.4167.

53. Malaysian Solar Resources Sdn. Bhd, "Photovoltaic module documentation MSR Standard")," 2010.

54. Z. A. Malek, "Lightning Awareness," 2017.